Published by :
https://www.ijert.org/
An International Peer-Reviewed Journal

International Journal of Engineering Research & Technology (IJERT)
ISSN: 2278-0181
Vol. 15 Issue 07 , July - 2026

Neural Network-Based Handover Timing Prediction for LEO Satellite NTN Links

Ghulam Muhayy Ud Din Qureshi[1], Tahir Hussain Nazir Hussain[2], Abid Jameel[3]
Saudi Telecom Operator

Abstract—Non-Terrestrial Networks (NTNs) extend the coverage of 5G New Radio (NR) through Low Earth Orbit (LEO) satellites, providing a resilient connectivity layer for remote regions and obstacle-dense, mass-gathering environments where terrestrial infrastructure may be congested, unavailable, or damaged. A key challenge in LEO NTN systems is the limited visibility period of each satellite. A satellite typically remains in view of a fixed ground location for only a few minutes before the connection must be transferred to another satellite. Moreover, the most suitable handover point varies significantly between passes because of differences in orbital geometry and maximum elevation. This paper develops a physically grounded model of a LEO satellite pass by combining orbital mechanics with linkbudget analysis. Publicly documented parameters of the Starlink constellation, including an orbital altitude of 550 km and an inclination of 53°, are used instead of purely assumed values. The model evaluates satellite elevation, slant range, Doppler shift, and signal-to-noise ratio (SNR) throughout representative passes over a ground location in Saudi Arabia. Using the generated pass data, a feedforward neural network is trained to estimate the remaining time before the satellite link falls below a usable SNR threshold. The model relies on noisy real-time telemetry measurements, including elevation angle, SNR, and Doppler shift. Its performance is evaluated against a fixed elevation-threshold method and a linear-regression baseline across 60 simulated satellite passes with varying geometries. The fixed-threshold baseline, calibrated using a single representative pass, performs poorly when applied to diverse pass conditions, producing an RMSE of 339.5 s. Linear regression reduces the RMSE to 27.1 s, while the neural network further lowers it to 9.3 s, representing an improvement of nearly three times over the linear baseline. The paper also discusses the practical implications for LEO NTN handover management, the limitations of a simulationbased study, and the requirements for future validation using real satellite telemetry.

Index Terms—5G NR, Non-Terrestrial Networks, NTN, LEO satellite, link budget, Doppler shift, handover, machine learning, neural network.

I. INTRODUCTION

Non-Terrestrial Networks (NTNs) integrate satellites, HighAltitude Platform Systems (HAPS), and unmanned aerial vehicles into the 5G New Radio (NR) ecosystem, extending connectivity to locations where terrestrial infrastructure is limited, damaged, or temporarily overloaded. Low Earth Orbit (LEO) satellite constellations are particularly suitable for this role because their relatively low orbital altitude results in lower propagation delay and free-space path loss than geostationary satellite systems. However, this advantage introduces an important operational challenge. Because LEO satellites move rapidly relative to the Earth's surface, an individual satellite remains visible to a fixed ground location for only a limited period before the connection must be transferred to another satellite.

This study is motivated by the digital-infrastructure objectives of Saudi Arabia's Vision 2030 [1], which emphasize reliable, resilient, and wide-area connectivity. Such connectivity is particularly important in remote regions, dense urban environments, and obstacle-dense mass-gathering locations, where terrestrial networks may experience severe congestion or temporary service disruption. In these scenarios, an NTN layer can provide supplementary or backup connectivity. Its effectiveness, however, depends on the network's ability to manage the short and highly variable visibility periods associated with LEO satellite passes.

The main engineering problem considered in this paper is satellite handover timing. A user equipment (UE) connected through a LEO satellite should transfer its connection to the next available satellite before the current link quality falls below an acceptable level. At the same time, initiating the handover too early reduces the usable duration of the existing link and may generate unnecessary signaling overhead. A simple handover strategy is to trigger the process when the satellite elevation angle falls below a predefined threshold. Although easy to implement, this method is usually calibrated using a representative satellite pass and may not perform consistently under different orbital geometries.

LEO satellite passes can vary considerably in maximum elevation, visibility duration, slant range, and received signal quality. A high-elevation or near-overhead pass may provide a strong link for several minutes, whereas a low-elevation grazing pass may remain close to the horizon and offer only a short period of usable connectivity. Consequently, a single elevation threshold may initiate handover too early during a strong pass or too late during a weaker pass, increasing the likelihood of interrupted service.

To address this limitation, this paper develops a combined orbital-mechanics and link-budget model of a LEO satellite pass using publicly documented constellation parameters. The model characterizes the variation of satellite elevation, slant range, Doppler shift, and signal-to-noise ratio (SNR) throughout each pass. A feedforward neural network is then trained to estimate the remaining time before the link falls below a defined usable SNR threshold using noisy real-time telemetry measurements. Its performance is evaluated against a fixed elevation-threshold method and a linear-regression baseline across a diverse set of simulated satellite passes.

II. BACKGROUND AND RELATED WORK

The development of 5G New Radio for Non-Terrestrial Networks began with the channel-model and use-case studies introduced in 3GPP Release 15, particularly through TR 38.811 [2]. The standard was later extended through dedicated

International Journal of Engineering Research & Technology (IJERT)
ISSN: 2278-0181
Vol. 15 Issue 07 , July - 2026

specifications, including TS 38.101-5 [3], to support user equipment operating over geostationary, medium Earth orbit, and low Earth orbit satellite systems. TR 38.811 provides the propagation, free-space path-loss, delay, and Doppler models that form the basis of the link-budget analysis developed in this study.

Hosseinian *et al.* [4] presented a comprehensive review of 5G NTN standardization and the main challenges associated with integrating satellite systems into terrestrial 5G networks. Their work highlights propagation delay, large Doppler shifts, mobility management, and synchronization as key technical issues. Sedin *et al.* [5] evaluated the throughput and capacity of 5G NR over LEO satellite links and demonstrated that rapidly changing satellite geometry has a direct effect on achievable system performance. More recently, Wong *et al.* [6] investigated satellite-to-device connectivity, interference, and performance in the context of 5G NR and future 6G systems, confirming that direct LEO connectivity remains an active area of research and development.

The orbital configuration considered in this paper is based on the publicly documented first operational shell of the Starlink constellation. The selected parameters, namely an orbital altitude of 550 km and an inclination of 53°, are consistent with the constellation configuration authorized by the U.S. Federal Communications Commission and reported in public technical documentation [7]. These values are used directly in the orbital simulation rather than being selected as arbitrary assumptions. As a basic validation step, the resulting model produces an orbital period of approximately 95.5 minutes and an orbital velocity of approximately 7.6 km/s, which are consistent with published values for satellites operating at this altitude.

The handover problem in LEO NTN differs substantially from conventional terrestrial mobility management. In terrestrial networks, handover decisions are generally driven by changes in signal strength caused by user movement between relatively fixed base stations. These changes are often gradual and depend on the user's speed, trajectory, and surrounding environment. In contrast, LEO satellite handovers are primarily caused by the rapid and predictable movement of satellites across the sky. Although satellite trajectories can theoretically be determined from orbital ephemeris data, practical handover decisions must often rely on noisy measurements, imperfect tracking information, and periodically updated network estimates.

Satellite handover management has been studied for several decades. Chowdhury *et al.* [9] reviewed handover techniques developed for early LEO mobile-satellite systems, while Papapetrou *et al.* [10] examined satellite handover strategies for maintaining service continuity in LEO constellations. Within the 5G NTN context, Juan *et al.* [8] proposed mobility and handover solutions for LEO satellite networks, and 3GPP TS 38.821 [14] documented the technical solutions considered for NR NTN mobility management.

Recent research has increasingly explored machinelearning-based approaches to improve satellite handover decisions. Dahouda *et al.* [16] proposed a learning-based handover framework intended to reduce excessive signaling during NTN mobility events. Yu *et al.* [12] developed a graphreinforcement-learning strategy for satellite handover selection, while Fan *et al.* [13] combined long short-term memory traffic prediction with an attention-enhanced reinforcementlearning framework. Demir *et al.* [17] evaluated the performance impact of different handover mechanisms in NTN systems and demonstrated that mobility-management design can significantly affect service continuity and overall network performance.

Most existing learning-based studies focus on satellite selection, resource allocation, traffic prediction, or handover scheduling. The present work addresses a narrower but complementary problem: predicting the remaining time before the current satellite link falls below a usable SNR threshold. The proposed method combines a physics-based orbital and linkbudget model with a learned multi-feature predictor that uses elevation, Doppler shift, and SNR measurements. The objective is to determine whether such an approach can generalize more effectively across different pass geometries than a fixed elevation-threshold rule calibrated using a single representative pass. This hybrid physics-and-learning methodology is conceptually related to the work of Neinavaie and Kassas [11], who combined analytical orbital models with machine learning for LEO satellite orbit prediction.

III. Technical Explanation

A satellite operating in a circular Low Earth Orbit at altitude h has an orbital radius

$$r = R_E + h, \tag{1}$$

where R_E is the mean radius of the Earth. Based on the standard two-body orbital-mechanics formulation [15], the orbital period is given by

$$T = 2\pi\sqrt{\frac{r^3}{\mu}}, \tag{2}$$

where μ denotes the Earth's standard gravitational parameter. For the Starlink Group-1 shell, with an orbital altitude of $h = 550$ km, the calculated orbital period is approximately 95.5 minutes. The corresponding orbital velocity is approximately 7.6 km/s, which is consistent with publicly reported values for this constellation [7].

As the satellite moves across the visible sky of a fixed ground station, its elevation angle increases from approximately 0° at acquisition of signal, reaches a maximum value, and then decreases back toward 0° at loss of signal. The maximum elevation depends on the minimum angular separation between the satellite ground track and the ground-station location. A near-overhead pass produces a high maximum elevation, whereas a grazing pass remains close to the horizon throughout its visibility period.

The slant range between the satellite and the ground station varies continuously during the pass. It reaches its minimum near the point of maximum elevation, where free-space path loss is lowest and the received signal-to-noise ratio is typically highest. As the satellite approaches the horizon, the slant range increases rapidly. This increase results in greater propagation loss, while the longer atmospheric path can introduce additional attenuation and further degrade link quality.

Rather than approximating the satellite pass using a predefined or symmetric elevation profile, this study calculates the geometry

International Journal of Engineering Research & Technology (IJERT)
ISSN: 2278-0181
Vol. 15 Issue 07 , July - 2026

directly from orbital dynamics. The satellite position is propagated in an Earth-Centered Inertial coordinate frame, while the ground-station position is updated to account for the Earth's rotation. The resulting relative position vector is then used to determine the time-varying elevation angle, slant range, radial velocity, Doppler shift, and link-budget parameters throughout each simulated pass.

IV. THEORETICAL BACKGROUND

A. LEO Orbital Geometry and Pass Characteristics

The satellite is modelled in a circular orbit with an inclination of 53°, while the position of the ground station is updated to account for the Earth's rotation at the sidereal angular rate. At each simulation time step, the satellite-to-ground relative position vector is transformed into the local coordinate frame of the ground station. The elevation angle is obtained from the projection of this vector onto the local vertical direction, while the slant range is calculated from its magnitude.

The relative radial velocity between the satellite and the ground station is determined from the time derivative of the slant range. This range rate governs the Doppler shift according to

$$f_D = -\frac{\dot{r}}{c} f_c, \tag{3}$$

where $\dot{r}$ is the slant-range rate, c is the speed of light, and f_c is the carrier frequency. The sign of f_D depends on whether the satellite is approaching or receding from the ground station. An approaching satellite produces a positive frequency offset under the adopted sign convention, whereas a receding satellite produces a negative offset.

For a representative Ka-band NTN downlink operating at 20 GHz [3], the simulation of a near-overhead pass produces Doppler shifts ranging from approximately −358 kHz to +448 kHz. These values are consistent with the severalhundred-kilohertz Doppler magnitudes reported for LEO Kaband links in the NTN literature [2]. The asymmetry between the minimum and maximum Doppler values arises from the combined effects of orbital geometry, Earth rotation, and the relative orientation of the satellite trajectory with respect to the ground station.

B. NTN Link-Budget Model

The link-budget model adopts a free-space path-loss formulation, consistent with the line-of-sight-dominant propagation conditions described in 3GPP TR 38.811 [2] for most of a satellite pass. The free-space path loss is calculated as

$$PL_{dB} = 20\log_{10}(d) + 20\log_{10}(f_c) - 147.55, \tag{4}$$

where d is the satellite-to-ground slant range in metres and f_c is the carrier frequency in hertz.

The received signal power is obtained by combining the free-space path loss with representative values for satellite effective isotropic radiated power, user-terminal antenna gain, and other link losses. The receiver noise power is calculated from the thermal noise density, channel bandwidth, and receiver noise figure. The instantaneous signal-to-noise ratio is therefore expressed as

$$\mathrm{SNR}_{dB} = P_{EIRP} + G_{RX} - PL_{dB} - L_{add} - N_{dB}, \tag{5}$$

where P_{EIRP} is the satellite EIRP, G_{RX} is the receivingantenna gain, L_{add} represents additional propagation and implementation losses, and N_{dB} is the receiver noise power.

The slant range changes continuously throughout each pass. For a 550 km LEO satellite, the range near the horizon can be several times greater than the minimum range reached during a high-elevation pass. This variation produces substantial changes in free-space path loss and, consequently, in the received SNR. The usable link duration is therefore determined by the evolving orbital geometry and link quality rather than by a fixed satellite-to-ground distance.

C. Handover-Timing Challenge and Machine-Learning Framework

A conventional handover policy may initiate a satellite switch when the elevation angle falls below a predefined threshold. Such a policy implicitly assumes that a particular elevation angle corresponds to a predictable remaining link duration. This assumption is only valid for passes with similar geometric characteristics.

In practice, satellite passes differ considerably in maximum elevation, slant range, radial velocity, and visibility duration. A near-overhead pass and a low-elevation grazing pass may reach the same elevation angle while having substantially different remaining times before link outage. Their range and range-rate profiles also differ, resulting in different SNRdegradation rates. Consequently, a threshold calibrated using one representative pass may initiate handover too early for another pass or too late to prevent service interruption.

This paper formulates handover timing as a supervised regression problem. At each observation instant, the objective is to estimate the remaining time before the received SNR falls below a predefined usability threshold. The predictor uses noisy telemetry features that may be available from the terminal or network, including elevation angle, SNR, Doppler shift, and their short-term rates of change.

A feedforward neural network is trained using data generated from multiple simulated passes with different orbital geometries and maximum elevation angles. Its performance is compared with two reference methods. The first is a naive physics-based baseline that extrapolates the remaining link duration from the current elevation angle and its rate of change while assuming a fixed elevation-based outage threshold. The second is a multivariable linear-regression model trained using the same telemetry features as the neural network.

The linear baseline is included to determine how much predictive improvement can be achieved through a simple learned correction of the telemetry measurements. The comparison with the neural network then isolates the additional benefit provided by nonlinear modelling of the relationship among elevation, SNR, Doppler shift, pass geometry, and remaining time to outage.

V. STUDY OBJECTIVES

A. Evaluate Practical Feasibility

The primary objective of this work is to evaluate the feasibility of using a learned correction model to predict LEO satellite

International Journal of Engineering Research & Technology (IJERT)
ISSN: 2278-0181
Vol. 15 Issue 07 , July - 2026

handover timing from noisy real-time telemetry. Its performance is compared with that of a fixed-threshold method calibrated using a single representative satellite pass.

B. Measure Key Performance Indicators

The study models the variation of satellite elevation, slant range, Doppler shift, and received SNR throughout representative LEO passes. Handover-timing performance is evaluated using the root-mean-square error (RMSE) and mean absolute error (MAE) of the predicted remaining time to link outage. These metrics are calculated for the naive elevationbased method, the linear-regression baseline, and the proposed neural-network model.

C. Validate Theoretical Predictions

Before applying the model to link-budget and handover analysis, the simulated orbital period and orbital velocity are compared with publicly reported values for the Starlink constellation. This comparison provides a basic validation of the orbital-mechanics implementation and confirms that the simulated satellite motion is physically realistic.

D. Identify Operational Challenges

The study investigates why a fixed elevation-threshold policy performs inconsistently across satellite passes with different maximum elevations and orbital geometries. It also quantifies the resulting handover-timing prediction error across a diverse set of simulated passes, including both low-elevation grazing passes and near-overhead passes.

E. Contribute Practical Design Guidelines

A further objective is to determine how much of the improvement in handover-timing accuracy is attributable to the use of a richer telemetry feature set and how much results from the neural network's nonlinear modelling capability. The comparison between linear regression and the neural network is intended to assess whether the additional computational complexity of the nonlinear model is justified by a meaningful improvement in prediction accuracy.

TABLE I: Simulation Configuration

Parameter	Specification
Orbital altitude	550 km (Starlink Group-1 shell)
Orbital inclination	53°
Ground station location	24.71°N, 46.68°E
Carrier frequency	20 GHz (Ka-band NTN downlink)
Channel bandwidth	50 MHz
Receiver noise figure	3 dB
SNR outage threshold	0 dB
Passes simulated	60 (varying RAAN/geometry)
Train / test split	42 / 18 passes
Total samples	12,370 (3,679 test)
ML model	Feed-forward NN, two hidden layers
Baseline methods	Elevation-threshold, linear regression

VI. Simulation Setup and Modelled Configuration

A. Test Environment

The ground station is positioned at a representative location in Saudi Arabia at 24.71°N latitude and 46.68°E longitude. The satellite is modelled using the publicly documented parameters of the Starlink Group-1 orbital shell, consisting of a circular orbit at an altitude of 550 km and an inclination of 53° [7].

A total of 60 satellite passes with different geometries are generated by varying the right ascension of the ascending node. This approach produces a broad range of pass conditions, from low-elevation grazing passes to near-overhead trajectories. The resulting dataset therefore captures substantial variation in maximum elevation, visibility duration, slant range, Doppler profile, and received SNR.

B. Equipment and Configuration

The simulation is implemented as a software-based orbital, link-budget, and machine-learning evaluation environment. The model propagates the satellite position, updates the ground-station position to account for Earth rotation, and calculates the time-varying elevation angle, slant range, range rate, Doppler shift, free-space path loss, and received SNR.

A representative Ka-band downlink carrier frequency of 20 GHz is used together with a 50 MHz channel bandwidth and a receiver noise figure of 3 dB. The usable-link boundary is defined by an SNR outage threshold of 0 dB. Samples generated before the descending link crosses this threshold are labelled with the true remaining time to outage and are used for training and evaluating the prediction models.

The 60 simulated passes are separated at the pass level rather than by randomly splitting individual samples. Fortytwo passes are used for model training, while the remaining 18 passes are reserved for testing. This arrangement prevents samples from the same satellite pass from appearing in both datasets and provides a more realistic assessment of how well each model generalizes to previously unseen pass geometries.

VII. DATA AND METHODOLOGY

All results presented in Section VIII are obtained from the orbital-mechanics and link-budget simulation described in the preceding sections. No live satellite telemetry is used in this study. The dataset-generation and evaluation procedure is summarized as follows.

1) Satellite-pass generation: For each of 60 selected right ascension of the ascending node (RAAN) values, the satellite elevation angle, slant range, Doppler shift, and received SNR are calculated at a fine temporal resolution from acquisition of signal to loss of signal. The simulations use the orbital and link parameters specified in Section VI. Pass configurations that do not provide a usable interval above the defined 0 dB SNR threshold are discarded and replaced, resulting in 60 usable passes spanning a wide range of maximum elevations, from low grazing trajectories to near-overhead passes.

2) Ground-truth target construction: For each usable pass, only samples on the descending portion of the trajectory, after the point of maximum SNR, are considered for handover prediction. At every sample instant, the true time to outage is defined as the remaining time until the received SNR first falls below the 0 dB usability threshold. This remaining duration constitutes the ground-truth regression target.

3) Telemetry-noise modelling: To represent imperfections in real-time satellite tracking and link-quality estimation, zeromean measurement noise is added to the simulated telemetry. The elevation measurements are corrupted with a standard deviation of 1°, the SNR measurements with a standard

International Journal of Engineering Research & Technology (IJERT)
ISSN: 2278-0181
Vol. 15 Issue 07 , July - 2026

deviation of 1.5 dB, and the Doppler measurements with a standard deviation of 2 kHz. Short-term rates of change for elevation, SNR, and Doppler shift are subsequently calculated from the noisy measurement sequences.

4) Prediction strategies: Three handover-timing prediction methods are evaluated: a *naive elevation-based method*, where the remaining time is estimated by extrapolating the current noisy elevation angle using its measured rate of change and assuming that link outage occurs at a fixed elevation threshold of 5°; a *linear-regression baseline*, a multivariable linearregression model trained using the complete noisy feature set, consisting of elevation, SNR, Doppler shift, and their short-term rates of change; and a *neural-network model*, a feedforward neural network with two hidden layers trained using the same input features as the linear model, learning the nonlinear relationship between the instantaneous telemetry, the evolving pass geometry, and the remaining time before link outage.

5) Training and testing procedure: The dataset is divided at the satellite-pass level to prevent observations from the same pass from appearing in both the training and testing sets. Data from 42 passes are used for model training, while 18 previously unseen passes are reserved for testing. This produces a total of 12,370 samples, of which 3,679 belong to the test set.

6) Performance evaluation: Prediction performance is assessed using root-mean-square error and mean absolute error:

$$\mathrm{RMSE} = \sqrt{\frac{1}{N}\sum_{i=1}^{N}\left(\hat{t}_i - t_i\right)^2}, \quad (6)$$

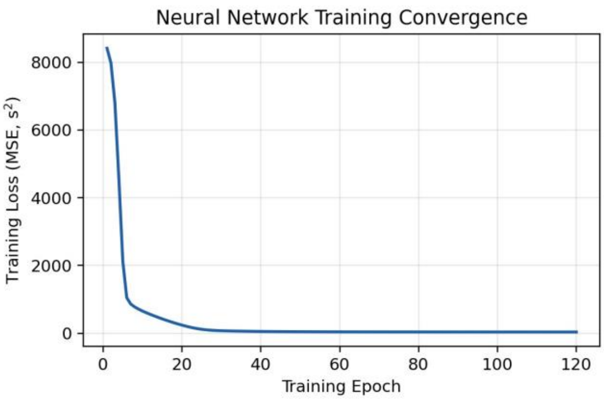

Fig. 1: Neural network training convergence (mean squared error vs. training epoch, with early stopping).

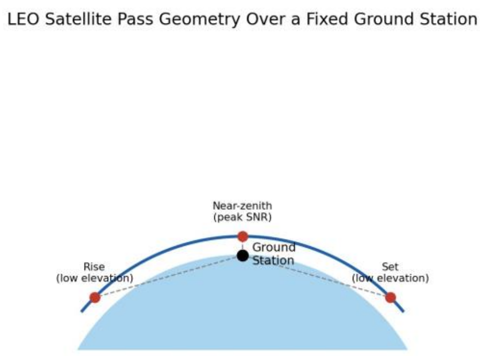

Fig. 2: LEO satellite pass geometry over a fixed ground station: elevation rises from acquisition of signal, through a maximum, back down to loss of signal.

$$\mathrm{MAE} = \frac{1}{N}\sum_{i=1}^{N}\left|\hat{t}_i - t_i\right|, \quad (7)$$

where t_i is the true remaining time to outage, $\hat{t}_i$ is the predicted value, and N is the number of test samples. RMSE gives greater weight to large timing errors, while MAE provides a direct measure of the average absolute prediction deviation.

The neural-network model is trained using the same complete feature set as the linear-regression baseline. The dataset is divided at the pass level, with 42 passes allocated for training and 18 passes reserved for testing. This approach ensures that samples from the same satellite pass do not appear in both subsets, thereby preventing information leakage and providing a more reliable measure of generalization to previously unseen pass geometries.

Fig. 1 presents the neural-network training-loss curve. All performance metrics reported in Section VIII are calculated exclusively using the 18 held-out test passes, none of which contributed samples during model training.

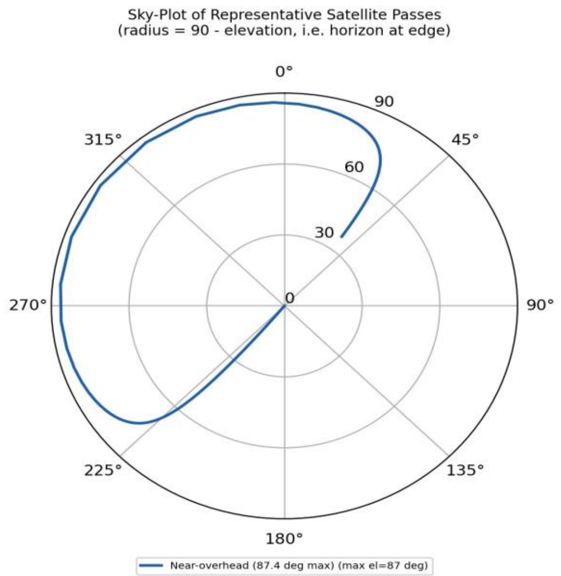

Fig. 3: Sky-plot of five representative simulated passes (radius = 90° minus elevation, so the horizon is at the outer edge and zenith is at the center),

International Journal of Engineering Research & Technology (IJERT)
ISSN: 2278-0181
Vol. 15 Issue 07 , July - 2026

illustrating the diversity of pass geometries the handover-timing model must generalize across.

VIII. RESULTS AND ANALYSIS

A. Modelled Pass Characteristics

Fig. 2 illustrates the geometry of a representative nearoverhead satellite pass with a maximum elevation angle of 87.4°. During this pass, the satellite remains above the local horizon for approximately 7.9 minutes. The slant range decreases as the satellite approaches its point of maximum elevation, reaching a minimum of approximately 550.5 km, and then increases as the satellite moves towards the horizon, reaching approximately 2700.5 km near acquisition and loss of signal.

Fig. 3 illustrates the geometric diversity represented in the simulated dataset. Some trajectories pass close to the ground station and reach elevations near the zenith, whereas others follow lower and shorter arcs with substantially smaller maximum elevation angles. These differences produce distinct slant-range, range-rate, Doppler, and SNR profiles.

This variation in pass geometry is the principal reason that a handover strategy based on a single fixed elevation threshold performs poorly across the full test set. The same elevation angle can correspond to substantially different remaining link durations depending on the satellite trajectory, maximum elevation, and rate of signal degradation. This effect is examined in greater detail in Section IX-A.

Fig. 4 shows elevation, SNR, and Doppler shift across this representative pass. SNR peaks near zenith at approximately 10.7 dB and falls to below the 0 dB usability threshold as elevation drops toward the horizon; Doppler shift crosses zero near the point of closest approach and reaches its largest magnitude, approximately 448 kHz, when the satellite is moving most directly toward or away from the ground station. Near

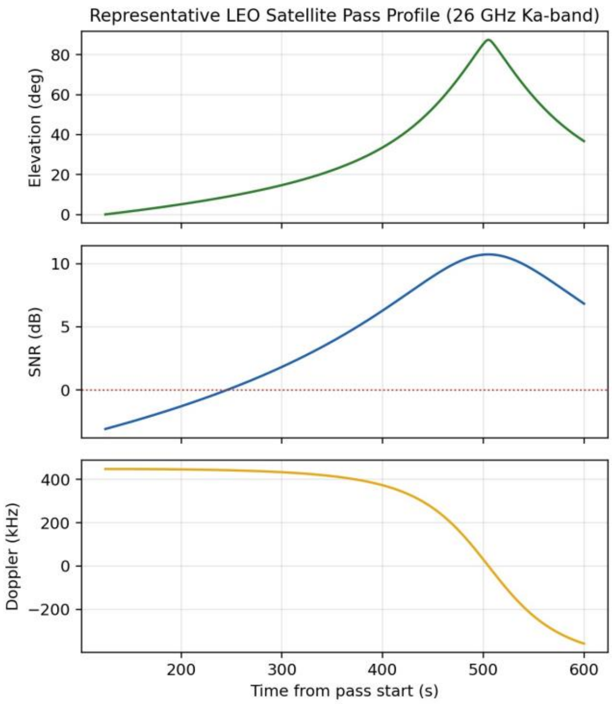

Fig. 4: Representative LEO satellite pass profile at 20 GHz: elevation, SNR, and Doppler shift vs. time from pass start.

TABLE II: Time-to-Handover Prediction Error by Strategy

Strategy	RMSE (s)	MAE (s)
Naive (elevation threshold)	339.5	263.1
Linear regression	27.1	21.6
Neural network	9.3	6.5

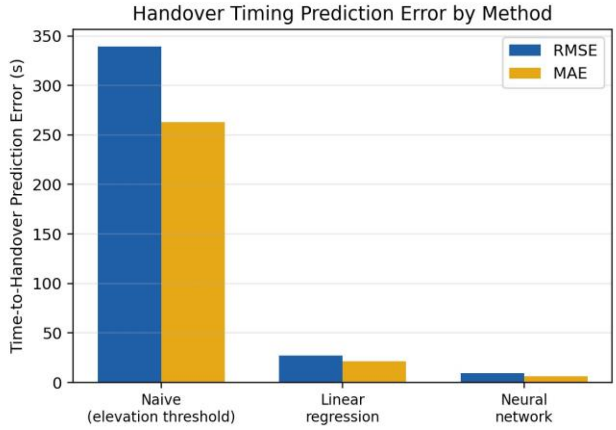

Fig. 5: Time-to-handover prediction error (RMSE and MAE) by strategy, evaluated on 18 held-out test passes (3,679 samples).

the point of closest approach, the radial component of velocity decreases and the Doppler shift passes through zero before changing sign as the satellite transitions from approaching to receding motion.

B. Handover-Timing Prediction

Table II and Fig. 5 summarize the prediction performance across the 18 held-out test passes. The naive fixed-threshold

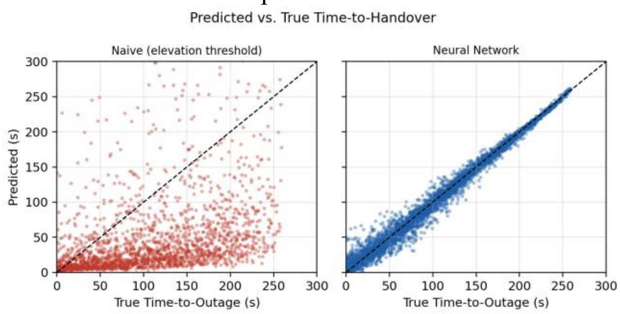

Fig. 6: Predicted vs. true time-to-outage for the naive and neural-network strategies on held-out test passes. The dashed line indicates perfect prediction.

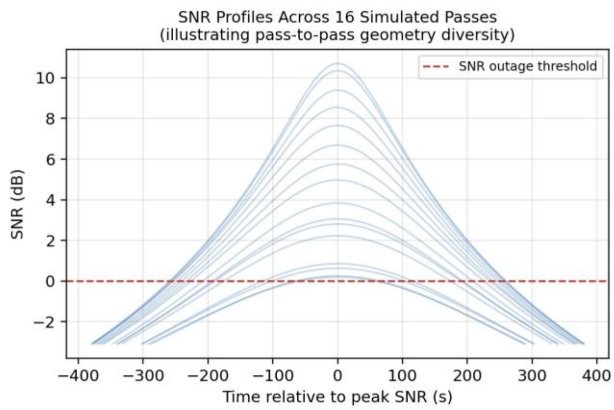

International Journal of Engineering Research & Technology (IJERT)
ISSN: 2278-0181
Vol. 15 Issue 07 , July - 2026

Fig. 7: SNR profiles across 16 of the 60 simulated passes, time-aligned to each pass's peak SNR, illustrating that passes differ substantially in how quickly SNR falls after the peak, undermining any fixed-threshold rule calibrated to a single pass shape.

strategy, calibrated using a single representative pass geometry, generalizes poorly to passes with different maximum elevations and range-rate profiles. It produces a root-mean-square error of 339.5 s, which is comparable to the duration of an entire LEO satellite pass and is therefore unsuitable for reliable handover-timing decisions.

The linear-regression baseline, which uses the richer telemetry feature set of elevation, SNR, Doppler shift, and their shortterm rates of change, reduces the RMSE to 27.1 s. This represents an improvement of more than one order of magnitude over the naive method. The result indicates that most of the achievable performance gain arises from incorporating linkquality and motion-related information rather than relying on elevation alone.

The neural-network model further reduces the RMSE to 9.3 s, representing an improvement of approximately three times relative to the linear-regression baseline. Because both learned models use the same input features, the remaining improvement can be attributed primarily to the neural network's ability to capture nonlinear relationships among satellite geometry, signal degradation, Doppler behavior, and remaining time to outage.

C. Trend Analysis

Fig. 7 illustrates the diversity of the post-peak SNR trajectories. Even after each pass is aligned relative to its own maximum-SNR point, the rate at which the link quality subsequently degrades varies considerably across the simulated passes. High-elevation passes generally retain usable SNR for longer periods and may exhibit a gradual initial decline, whereas lower grazing passes experience shorter usable intervals and more rapid degradation.

This variation confirms that the remaining time to outage cannot be inferred reliably from a single instantaneous elevation value. Two passes observed at the same elevation angle may have different slant ranges, radial velocities, Doppler shifts, and SNR slopes, leading to substantially different outage times. The richer telemetry features therefore provide information about both the current link condition and the direction and rate at which it is evolving.

The linear-regression model captures much of this additional information and corrects the large systematic errors produced by the fixed-threshold strategy. However, the relationship between the measured features and the remaining link duration is not entirely linear. The neural network provides a further reduction in error by modelling interactions such as elevationdependent range variation, nonlinear free-space path-loss behavior, and pass-specific SNR-degradation patterns.

Some passes approach the outage threshold within approximately one minute of reaching peak SNR, whereas others remain above the usable threshold for several additional minutes. A fixed elevation threshold calibrated to any single pass profile is therefore inherently mismatched when applied to passes with different geometric and link-quality characteristics.

Fig. 6 compares the predicted and true time to outage for the naive and neural-network strategies. The naive method exhibits a broad and structured dispersion around the ideal diagonal, indicating systematic prediction errors rather than purely random variation. In particular, the method fails to distinguish reliably between passes with different elevation, slant-range, and range-rate profiles.

By contrast, the neural-network predictions are concentrated much more closely around the ideal diagonal across the full range of target values. This behavior indicates that the model has learned a relationship that generalizes across different pass geometries rather than fitting only a limited subset of the training data. The result also supports the use of combined telemetry features, since elevation, SNR, Doppler shift, and their rates of change jointly provide a more complete representation of the current link state.

IX. DISCUSSION

A. Theoretical and Practical Alignment

The large prediction error produced by the naive strategy is a direct consequence of treating elevation angle as a sufficient indicator of remaining link quality. In practice, two satellite passes may cross the same elevation angle while having substantially different times remaining before outage. This difference depends on the pass geometry, slant range, radial velocity, maximum elevation, and rate of SNR degradation.

The linear-regression model recovers most of the achievable improvement by incorporating SNR, Doppler shift, and shortterm rates of change in addition to elevation. This result suggests that the dominant relationship between observable telemetry and time to outage can be represented reasonably well using a simple multivariable model.

The neural network provides a further reduction in prediction error, indicating that the relationship is not entirely linear. This nonlinear component may arise from the geometric relationship between elevation and slant range, the logarithmic dependence of path loss on distance, and the asymmetric variation of range rate and SNR near the horizon. The comparison therefore shows that richer telemetry provides the largest improvement, while nonlinear modelling contributes an additional but smaller performance gain.

B. System Limitations

The results of this study are based entirely on orbitalmechanics and link-budget simulation and have not yet been validated using live satellite telemetry. The satellite orbit is represented as circular and is propagated without modelling perturbations such as atmospheric drag, Earth oblateness, orbital eccentricity, or long-term ephemeris error. Although these effects are relatively small over an individual pass, they may become important in long-duration tracking or operational prediction systems.

The link-budget model assumes free-space path loss and does not explicitly account for atmospheric absorption, rain attenuation, shadowing, antenna misalignment, polarization loss, interference, or adaptive beamforming behavior. These effects may be particularly important for a Ka-band downlink, especially under adverse weather conditions or at low elevation angles.

The study also uses representative values for satellite EIRP, terminal antenna gain, receiver noise figure, and channel

International Journal of Engineering Research & Technology (IJERT)
ISSN: 2278-0181
Vol. 15 Issue 07 , July - 2026

bandwidth rather than measurements from a specific commercial NTN system. Similarly, the added measurement noise is a stylized approximation of tracking and estimation errors and has not been calibrated against a particular receiver or network implementation.

Although the 60 simulated passes cover a broad range of maximum elevations and orbital geometries, they may not represent every condition encountered in practice. Examples include extremely low grazing passes, partial blockage, rapidly changing interference, intermittent beam availability, and scenarios in which the target satellite is not immediately replaced by a suitable neighbouring satellite. The reported results should therefore be interpreted as evidence of relative model behavior under controlled conditions rather than as a direct estimate of field performance.

C. Deployment Implications

The magnitude of the naive method's error, which is comparable to the duration of an entire satellite pass, indicates that a fixed elevation-threshold policy is unsuitable as the sole basis for handover timing in a LEO NTN system operating across diverse pass geometries. Such variation would be expected in deployments serving users at different locations, latitudes, look angles, and orbital-track offsets.

A telemetry-based prediction model can provide a more adaptive estimate of the remaining usable link duration. The strong performance of the linear-regression baseline is operationally important because it suggests that a lightweight model may deliver most of the available benefit with limited computational and implementation complexity. Such a model could be suitable for terminals or network nodes with strict processing, power, or latency constraints.

The neural network provides an additional improvement where higher timing accuracy is required. An RMSE of 9.3 s may allow the network to initiate handover preparation closer to the actual outage point while maintaining an appropriate safety margin. This could reduce premature handovers, preserve more usable connection time, and lower unnecessary signaling.

In an operational system, the predicted time to outage would not necessarily act as the sole handover trigger. It could instead be combined with target-satellite availability, beam load, propagation delay, service priority, and handover execution time. The prediction could also be used to initiate preparatory actions, such as target selection, resource reservation, synchronization, or measurement reporting, before the current link reaches its critical threshold.

D. Potential Improvements

Several extensions could improve the realism and practical relevance of the proposed framework. First, the orbital model could incorporate perturbation effects such as atmospheric drag, Earth oblateness, orbital eccentricity, and ephemeris uncertainty. Although these effects are limited over the duration of a single pass, they become increasingly important in longterm tracking and prediction studies.

Second, the link-budget model could be extended beyond free-space path loss to include atmospheric absorption, rain attenuation, shadowing, antenna-pointing loss, polarization mismatch, and interference. These effects are particularly relevant for Ka-band links and at low elevation angles, where the atmospheric propagation path is considerably longer. The propagation framework described in 3GPP TR 38.811 [2] provides a suitable basis for such an extension.

Third, the measurement-noise parameters should be calibrated using actual UE-side tracking, Doppler-estimation, and channel-quality measurement data. The current noise model is intentionally stylized and does not capture possible temporal correlation, measurement bias, or receiver-specific behavior.

Finally, the most important next step is validation using real satellite-pass telemetry. Evaluating the trained model against measured elevation, Doppler, SNR, and link-outage events would determine whether the improvements observed in simulation remain valid under operational channel conditions and hardware limitations.

X. CONCLUSION

This paper developed an integrated orbital-mechanics and link-budget model of a LEO satellite pass using publicly documented Starlink constellation parameters. The model was used to study the handover-timing challenge created by the short and highly variable visibility windows associated with LEO NTN connectivity.

A fixed elevation-threshold strategy calibrated using a single representative pass performed poorly across diverse pass geometries, producing a root-mean-square timing error comparable to the duration of an entire satellite pass. A linearregression model using elevation, SNR, Doppler shift, and their short-term rates of change reduced the RMSE to 27.1 s, demonstrating that most of the available improvement results from using richer telemetry rather than elevation alone. The feedforward neural network reduced the RMSE further to 9.3 s, representing an improvement of nearly three times over the linear baseline.

The results therefore support a bounded conclusion. The largest performance gain comes from incorporating additional link and motion information, while nonlinear modelling provides a smaller but measurable improvement. This distinction is important for deployment design because it suggests that a lightweight linear model may be sufficient for resourceconstrained terminals, whereas a neural-network predictor may be justified where higher handover-timing accuracy is required.

Within the broader objectives of Saudi Vision 2030 [1], a well-managed LEO NTN layer could strengthen connectivity resilience in remote areas, dense urban environments, and mass-gathering locations where terrestrial capacity may become congested or temporarily unavailable. However, the results indicate that such deployments should account explicitly for the diversity of satellite-pass geometries rather than relying solely on fixed elevation thresholds.

The present conclusions are based on simulation and should not be interpreted as direct field-performance measurements. Validation using real satellite telemetry, realistic atmospheric propagation, and operational handover procedures remains the most important step toward confirming the practical value of the proposed approach.

ACKNOWLEDGMENT

All research-design decisions, modelling assumptions, simulation procedures, and analytical interpretations were developed and verified by the authors. AI-assisted tools were used solely to support language refinement, simulation-code organisation, and document formatting. The authors retained full responsibility for the technical content, validation, and conclusions presented in this paper.

REFERENCES

[1] Kingdom of Saudi Arabia, "Saudi Vision 2030." [Online]. Available: https://www.vision2030.gov.sa

[2] 3GPP TR 38.811, "Study on New Radio (NR) to support non-terrestrial networks," Release 15, 2020.

[3] 3GPP TS 38.101-5, "NR; User Equipment (UE) radio transmission and reception; Part 5: Satellite access Radio Frequency (RF) requirements."

[4] M. Hosseinian, J. P. Choi, S.-H. Chang, and J. Lee, "Review of 5G NTN standards development and technical challenges for satellite integration with the 5G network," *IEEE Aerosp. Electron. Syst. Mag.*, vol. 36, pp. 22–31, 2021.

[5] J. Sedin, L. Feltrin, and X. Lin, "Throughput and capacity evaluation of 5G new radio non-terrestrial networks with LEO satellites," in *Proc. IEEE Global Commun. Conf. (Globecom)*, 2020.

[6] O. S. Wong, M. A. Gregory, and S. Li, "Integration of non-terrestrial network for 5G NR and future 6G: LEO satellite-to-device performance and interference analysis," *Computer Networks*, vol. 275, art. 111870, Feb. 2026.

[7] eoPortal, "Starlink Satellite Constellation." [Online]. Available: https://www.eoportal.org/satellite-missions/starlink

[8] E. Juan, M. Lauridsen, J. Wigard, and P. Mogensen, "Handover solutions for 5G low-earth orbit satellite networks," *IEEE Access*, vol. 10, 2022.

[9] P. K. Chowdhury, M. Atiquzzaman, and W. Ivancic, "Handover schemes in satellite networks: state-of-the-art and future research directions," *IEEE Commun. Surveys Tuts.*, vol. 8, no. 4, pp. 2–14, 2006.

[10] E. Papapetrou, S. Karapantazis, G. Dimitriadis, and F.-N. Pavlidou, "Satellite handover techniques for LEO networks," *Int. J. Satell. Commun. Netw.*, vol. 22, no. 2, pp. 231–245, 2004.

[11] M. Neinavaie and Z. M. Kassas, "A hybrid analytical-machine learning approach for LEO satellite orbit prediction," in *Proc. 25th Int. Conf. Information Fusion*, 2022, pp. 1–7.

[12] H. Yu, W. Gao, and K. Zhang, "A graph reinforcement learningbased handover strategy for low earth orbit satellites under power grid scenarios," *Aerospace*, vol. 11, art. 511, 2024.

[13] D. Fan, S. Zhou, J. Luo, Z. Yang, and M. Zeng, "Joint traffic prediction and handover design for LEO satellite networks with LSTM and attention-enhanced Rainbow DQN," *Electronics*, vol. 14, art. 3040, 2025.

[14] 3GPP TS 38.821, "Solutions for NR to support non-terrestrial networks (NTN)," 2024.

[15] D. A. Vallado, *Fundamentals of Astrodynamics and Applications*, 4th ed. Microcosm Press/Springer, 2013.

[16] M. K. Dahouda, S. Jin, and I. Joe, "Machine learning-based solutions for handover decisions in non-terrestrial networks," *Electronics*, vol. 12, no. 8, art. 1759, 2023.

[17] Y. I. Demir, M. S. J. Solaija, and H. Arslan, "On the performance of handover mechanisms for non-terrestrial networks," arXiv:2201.04904, 2022.